Manipulation of light with α transformation media

Wei Yan, Min Yan, and Min Qiu*

Laboratory of Optics, Photonics and Quantum Electronics, Department of Microelectronics and Applied Physics, Royal Institute of Technology (KTH), Electrum 229, 16440 Kista, Sweden
**Corresponding author: min@kth.se*

Received February 14, 2011; accepted March 26, 2011;
posted April 4, 2011 (Doc. ID 142654); published May 17, 2011

A type of transformation media called α media is proposed by performing a direct transformation to the metric tensor of another kind of media, called seed media. Light rays in an α medium correlate to those in its seed medium through a simple displacement or rotation relation. Three types of commonly encountered anisotropic media are covered by the concept of α media: (1) media of slab shape, having continuous translational symmetry with respect to two Cartesian coordinate components; (2) media of cylindrical shape, having cylindrical rotational symmetry and continuous translational symmetry along the longitudinal direction; (3) media of spherical shape, having spherical rotational symmetry, with two principal axes along the symmetry directions, and with the material parameters in the same sign. Optical properties of such media can be effectively interpreted through recalling the properties of certain isotropic media, i.e., their seed media. Conversely, from simple isotropic media in which light trajectories are well known, one can design α media for manipulating light. Based on this fact, several optical devices, including frequency demultiplexers, beam splitters, focusing lenses, and radiation controllers, are designed and numerically verified. The famed invisibility cloak derived from a conventional coordinate transformation is revisited from the α media perspective.

OCIS codes: 230.3205, 080.5692.

1. INTRODUCTION

Transformation optics, a recently booming area in optics, opens a new window to designing optical devices for manipulating light [1–18]. The physical foundation of transformation optics relies on the covariant form of Maxwell's equations. Either the curved coordinate system or curved space–time can be emulated by special media called transformation media. By applying the principle of transformation optics, a lot of interesting applications are proposed, such as invisibility cloaks [1–11], electromagnetic (EM) wormholes [12], superlenses [13–15], optical illusion devices [16], and transmutation of device singularities [17]. Transformation optics also gives a geometrical insight into some well-known phenomena, such as negative index lenses [3] and complementary media [13].

For transformation optics, the coordinate transformation is the most popular approach to designing transformation media, because it offers an elegant geometrical path to the design. However, two limitations are inherent in this approach: (1) material parameters of transformation media are always reciprocal with $\epsilon = \mu$; (2) transformation media and their original space have the same curvature property. To overcome the first limitation, Bergamin proposed an extended coordinate transformation approach by assigning different transformed spaces to the field set (electric field **E** and magnetic induction **B**) and the field set (electric displacement field **D** and magnetic induction **H**), respectively [18]. In essence, such an extended approach still belongs to the coordinate transformation.

In the present paper, we propose an approach different from the coordinate transformation for designing transformation media. In our approach, the second limitation of the coordinate transformation does not exist anymore. The paper is organized as follows. In Section 2, we construct α media by applying a transformation to the metric tensor directly and compare the difference between our transformation and the coordinate transformation. In Section 3, within the framework of ray optics, we study the characteristics of light trajectories in the α media. In Section 4, material parameters of the α media are discussed. In Section 5, based on the α media, several optical devices are proposed and numerically verified. In Section 6, invisibility cloaks derived from coordinate transformations are revisited from the α media perspective. Finally, the conclusion to the paper is given in Section 7.

2. TRANSFORMATION RELATION AND TRANSFORMATION MEDIA

Consider a space with the spatial metric tensor g^s_{ij} ($i, j = 1, 2, 3$). The spatial coordinates of such a space are (x^1, x^2, x^3). This space is called *seed space*. Based on the seed space, a new space called *α space* with the metric tensor g^α_{ij} is constructed by the following transformation relation expressed as

$$g^\alpha = \mathrm{diag}[\alpha, 1, 1] g^s \mathrm{diag}[\alpha, 1, 1], \tag{1}$$

where g^s and g^α represent the matrix forms of the metric tensors g^s_{ij} and g^α_{ij}. The spatial coordinates in the two spaces have the same range under the above-defined transformation relation.

In the present paper, we assume that any component of g^s_{ij} and g^α_{ij} is either a constant or a function depending on one specified coordinate component, which is chosen to be x^1. Such an assumption indicates that the two spaces have the same translational or rotational symmetry concerning coordinate components x^2 and x^3. Respecting such symmetry, the boundary of the seed and α spaces is set to be a closed surface with $x^1 = a_1$ or two separated surfaces with $x^1 = a_1$ and $x^1 = a_2$, where a_1 and a_2 are two arbitrary constants.

According to transformation optics, it is known that a space with a certain metric tensor is equivalent to certain transformation media in the laboratory space [4]. Transformation media corresponding to the seed space and the α space are called *seed media* and *α media*, respectively. In the laboratory space, we interpret (x^1, x^2, x^3) as a right-handed coordinate system with the metric tensor g^c_{ij}. In such a coordinate system, the material parameters of the seed and α media are expressed as

$$\epsilon^s = \mu^s = \pm\frac{\sqrt{\det(g^s)}}{\sqrt{\det(g^c)}} h(g^s)^{-1} g^c h^{-1}, \tag{2}$$

$$\epsilon^\alpha = \mu^\alpha = \pm\frac{\sqrt{\det(g^\alpha)}}{\sqrt{\det(g^c)}} h(g^\alpha)^{-1} g^c h^{-1}, \tag{3}$$

respectively, where g^c represents the matrix form of the metric tensor g^c_{ij}; $h = \mathrm{diag}[\sqrt{g^c_{11}}, \sqrt{g^c_{22}}, \sqrt{g^c_{33}}]$; $\pm$ represents the handedness of (x^1, x^2, x^3) in the seed or α space (+ for a right-handed coordinate system, and – for a left-handed coordinate system).

Before ending this section, we compare the difference between our transformation defined in Eq. (1) and the coordinate transformation. For the coordinate transformation, one cannot transform a flat (curved) space to a curved (flat) space. However, such transformation is permitted here. As an example, consider a two-dimensional (2D) case. The seed space is a flat space with $g^s = \mathrm{diag}[1, r^2]$. Its Gaussian curvature, K, is equal to zero. Applying the defined transformation relation to the seed space with $\alpha = r^2$, the α space is obtained with $g^\alpha = \mathrm{diag}[r^2, r^2]$. The α space becomes curved, and its Gaussian curvature, K, is equal to $1/r^4$.

3. LIGHT RAYS IN SEED AND α MEDIA

Consider a seed medium put in an arbitrary background. In this paper, our emphasis is on light ray characteristics within the medium; any reflection at the boundary interface is therefore ignored. As discussed in Section 2, we know that the boundary of the seed medium is a closed continuous surface with $x^1 = a_1$ or two separated surfaces with $x^1 = a_1$ and $x^1 = a_2$. A light ray from the background is incident on the seed medium at the boundary $x^1 = a_1$ and leaves the boundary $x^1 = a_i$, where $i = 1$ or 2. It is assumed that the refracted ray in the seed medium follows the equations

$$x^1 = f_1(\sigma), \qquad x^2 = f_2(\sigma), \qquad x^3 = f_3(\sigma), \tag{4}$$

where σ has a range of $\sigma \in [\sigma_1, \sigma_2]$, and σ_1 and σ_2 are two constants.

Replacing the seed medium by the corresponding α medium, it can be proven (Appendix A) that the refracted light ray in the α medium follows the trajectory

$$\begin{aligned} x^1 &= f_1(\sigma), \\ x^2 &= \int_{\sigma_1}^{\sigma} \alpha(x^1)\frac{df_2(\sigma)}{d\sigma}\mathrm{d}\sigma + f_2(\sigma_1), \\ x^3 &= \int_{\sigma_1}^{\sigma} \alpha(x^1)\frac{df_3(\sigma)}{d\sigma}\mathrm{d}\sigma + f_3(\sigma_1), \end{aligned} \tag{5}$$

where the parameter σ has the same range as that in Eq. (4).

Consider a special case when α is a constant. Equation (5) is simplified to

$$\begin{aligned} &x^1 = f_1(\sigma), \qquad x^2 = \alpha f_2(\sigma) - \alpha f_2(\sigma_1) + f_2(\sigma_1), \\ &x^3 = \alpha f_3(\sigma) - \alpha f_3(\sigma_1) + f_3(\sigma_1). \end{aligned} \tag{6}$$

Denote Δx^{is} and $\Delta x^{i\alpha}$ as the coordinate changes of the light ray passing through the seed medium and the α medium, respectively. From Eqs. (4) and (6), one derives that

$$\Delta x^{1\alpha} = \Delta x^{1s}, \qquad \Delta x^{2\alpha} = \alpha\Delta x^{2s}, \qquad \Delta x^{3\alpha} = \alpha\Delta x^{3s}, \tag{7}$$

where α is a constant. When α is a negative value, Δx^{2s} (Δx^{3s}) and $\Delta x^{2\alpha}$ ($\Delta x^{3\alpha}$) have different signs. This implies that light experiences positive refraction in one medium and negative refraction in the other.

Let us also look at the phase changes of the light ray passing through the seed and α media, which are denoted as $\Delta\phi^s$ and $\Delta\phi^\alpha$, respectively. When α is a constant, one has (Appendix B)

$$\Delta\phi^\alpha = \alpha\Delta\phi^s. \tag{8}$$

Equation (8) clearly shows that $\Delta\phi^s$ and $\Delta\phi^\alpha$ have different values. In contrast, in the case of coordinate transformation, the phase change is a conserved quantity, because it is a scalar independent of any coordinate transformation. For a more general case, where α is not a constant, the relationship between $\Delta\phi^s$ and $\Delta\phi^\alpha$ is expressed in Eq. (B2). The same conclusion holds.

In this section, we have demonstrated that light rays in an α medium and its seed medium can be correlated through a simple displacement or rotation relationship determined by the parameter α, which we refer to as the *α-relation*. By adjusting the parameter α, light rays in the α medium can be adjusted accordingly.

4. MATERIAL PARAMETERS OF α MEDIA

The α media show a potential for controlling light by adjusting the parameter α. At first sight, it seems that their material parameters are complicated. However, in the following, it will be shown that such media can be designed with achievable, simple material parameters and cover several types of commonly encountered anisotropic media.

Consider g^s and g^α with only diagonal components and $g^s = n^2 g^c$, where n is a real constant or function. In this case, the seed medium is found to be isotropic, while the α medium is anisotropic. Their material parameters are

$$\epsilon^s = \mu^s = n, \tag{9}$$

$$\epsilon^\alpha = \mu^\alpha = n\,\mathrm{diag}[1/\alpha, \alpha, \alpha], \tag{10}$$

where $n^2 g^c$ and α are independent of x^2 and x^3, because g^s and g^α are independent of x^2 and x^3 by the assumption proposed in Section 2.

A. α Media in Cartesian, Cylindrical, and Spherical Coordinate Systems

Consider the α medium in a Cartesian coordinate system with $g^c = \mathrm{diag}[1, 1, 1]$. The material parameters of the α medium in Eq. (10) require that α and n be constants or depend on only one Cartesian coordinate. Additionally, the geometry shape of the α medium is a slab, owing to the boundary requirement as discussed in Section 2.

Consider the α medium in a cylindrical coordinate system with $g^c = \mathrm{diag}[1, r^2, 1]$ and coordinates denoted by (r, θ, z). The α medium requires α and n to be independent of θ and z. The geometrical shape of the α medium is a cylinder.

Consider the α medium in a spherical coordinate system with $g^c = \mathrm{diag}[1, r^2, r^2 \sin^2\theta]$ and coordinates denoted by (r, θ, ϕ). It seems that one can not find a proper n and α to construct an α medium, because g^c depends on both r and θ. However, the anisotropic media expressed in Eq. (10) with spherical rotational symmetry, i.e., n and α independent of angular coordinates, are qualified α media. To show this, we note that the light trajectory in an anisotropic medium with spherical rotational symmetry can always be found to lie in a flat plane passing through the origin. Such a plane can be described by a radial coordinate, r, and an angular coordinate, ϕ, with a range of $[0, 2\pi]$. Accordingly, its metric tensor is $\mathrm{diag}[1, r^2]$, just as in a 2D cylindrical coordinate system. In this sense, this three-dimensional (3D) spherical case is equivalent to a 2D cylindrical case. Thus, anisotropic media expressed in Eq. (10) with spherical rotational symmetry are α media. The geometry shape of the α medium is a sphere.

In Fig. 1, a light ray passing through the above-mentioned three types of α media and the corresponding seed media is illustrated. It is seen that the light ray is displaced or rotated in the α media as compared with the light ray in their seed media.

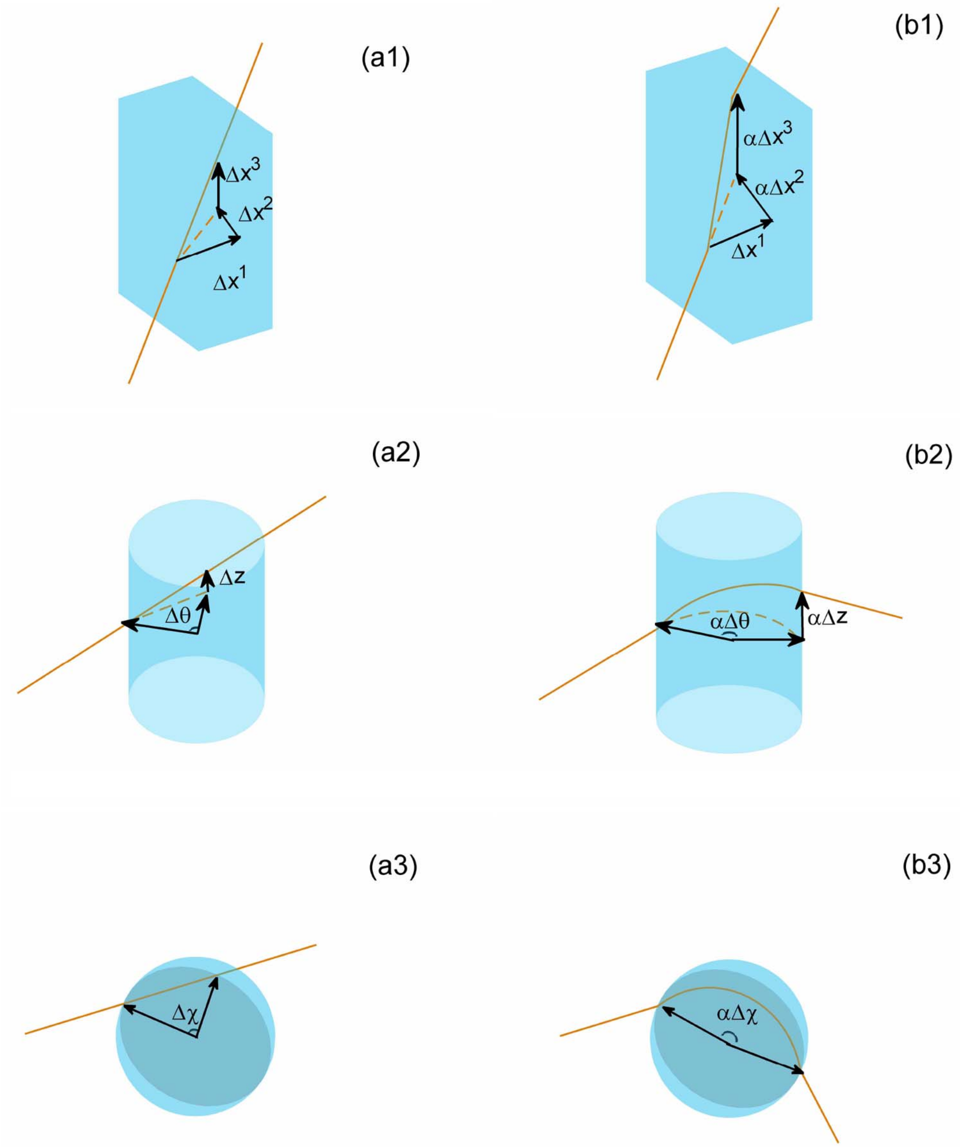

Fig. 1. (Color online) Illustration of a light ray passing through three types of α media and the corresponding seed media. The material parameters of seed and α media are expressed in Eqs. (9) and (10), respectively. (a1) and (b1) represent the seed medium and α medium, respectively, with the three principal axes being Cartesian axes, (a2) and (b2) represent the seed medium and α medium, respectively, with the three principal axes being cylindrical axes; (a3) and (b3) represent the seed medium and α medium, respectively, with the three principal axes being spherical axes. The background and the seed media are all set to be free space, and the parameter α is set to be a constant.

B. Simplification of α Media

In the above section, the material parameters of α media in Cartesian, cylindrical, and spherical coordinate systems are discussed. Even though the material parameters have a relatively simple form, they are still restricted by the conditions $\epsilon^\alpha = \mu^\alpha$, $\epsilon^\alpha_{x^2} = \epsilon^\alpha_{x^3}$, and $\mu^\alpha_{x^2} = \mu^\alpha_{x^3}$, which make the fabrication of the α media difficult. In this section, we will lift these restrictions by using some simplifications.

Light in different media with the same dispersion relation undergoes the same trajectory in the geometrical optics limit. This indicates that one can simplify the α media by keeping the dispersion relation intact, such that the requirement of $\epsilon^\alpha = \mu^\alpha$ can be relaxed. If one is interested in light with a particular polarization, the simplification can be carried further. As an example, consider a light propagating in the $x^1 - x^2$ plane with TE polarization (electrical fields have only an x^3 component). In this case, the material parameters of the α medium in Eq. (10) can be simplified to $\mu_{x^1} = n_2/\alpha$, $\mu_{x^2} = n_2\alpha$, and $\epsilon_{x^3} = n_1\alpha$, where $n_1 n_2 = n^2$, and the permittivity can be simply isotropic. On the other hand, an anisotropic medium with material parameters μ_{x^1}, μ_{x^2}, and ϵ_{x^3} of the same sign can be viewed as a simplified or an ideal α medium. Such a medium has an α-relation with an isotropic medium with a refractive index of $n = \sqrt{\epsilon_{x^3}\mu_{x^1}}$. The parameter α is equal to $\mathrm{sgn}\sqrt{\mu_{x^2}/\mu_{x^1}}$, where sgn $= 1$ when the material parameters are positive and sgn $= -1$ when they are negative. For TM-polarized light or light propagating in the $x^1 - x^3$ plane, one can obtain similar results. The generalized results are given in Table 1.

Applying the simplification principle, we simplify three types of α media in Cartesian, cylindrical, and spherical coordinate systems as discussed in Section 4.A.

1. In a Cartesian coordinate system, consider light propagating in the $x^1 - x^2$ plane. The simplified α media, of slab shape with the boundary $x^1 =$ constant, only require continuous translational symmetry concerning two Cartesian coordinates, x^2 and x^3 (material parameters are independent of x^2 and x^3).
2. In a cylindrical coordinate system, consider light propagating in the $r - \theta$ or $r - z$ plane. The simplified α media, of cylindrical shape, only require cylindrical rotational symmetry and continuous translational symmetry along z (material parameters are independent of θ and z).
3. In a spherical coordinate system, consider light propagating in an arbitrary flat plane passing the origin. The simplified α media, of spherical shape, only require spherical rotational symmetry.

It is noticed that the above-mentioned three types of simplified media have material parameters with the same sign and principal axes coinciding with the corresponding coordinate axes. Their seed media are isotropic media, because they inherit from their ideal media. Light propagating in such media can be understood by evocating its trajectory in the corresponding isotropic seed media plus an α-relation. From the device design point of view, one can therefore realize complex light propagation in a (simplified) α medium based on simple light trajectories in well-understood isotropic media. Additionally, such media are commonly encountered anisotropic media, and can be fabricated by the current technology of metamaterials.

5. OPTICAL DEVICES BASED ON α MEDIA

In this section, several optical devices will be demonstrated based on the α media in a cylindrical coordinate system. We focus on light propagation in the r–θ plane with TE polarization. The devices for TM operation can be obtained similarly. Additionally, by the same principle, we can also design similar optical devices based on the α media in the other coordinate systems, such as Cartesian and spherical coordinate systems.

A. Frequency Demultiplexer

Consider a cylinder made of a positive homogenous medium. The material components μ_r, μ_θ, and ϵ are independent of z and θ. As discussed in Section 4.B, it is known that such an anisotropic medium has the α-relation with an isotropic medium, which has a refractive index of $n = \sqrt{\mu_r \epsilon}$. The parameter α is equal to $\sqrt{\mu_\theta/\mu_r}$. From Eq. (7), one knows that $\Delta\theta^\alpha = \alpha\Delta\theta^s$, where $\Delta\theta^\alpha$ and $\Delta\theta^s$ represent the angular change for a light ray passing through an α medium and its corresponding seed medium, respectively. Manifestly, this cylinder can operate as a frequency demultiplexer if $\Delta\theta^\alpha$ depends on the frequency. Because $\alpha = \sqrt{\mu_\theta/\mu_r}$, the dispersive μ_θ can make this happen. The components μ_r and ϵ are designed to be nondispersive, which makes $\Delta\theta^s$ frequency-independent. Thus, $\Delta\theta^\alpha$ at different angular frequencies, ω, is expressed as

$$\Delta\theta^\alpha(\omega) = \sqrt{\frac{\mu_\theta(\omega)}{\mu_r}}\Delta\theta^s. \tag{11}$$

To demonstrate this application, we consider an example in which the cylinder is composed of a medium with $\mu_r = 1$, $\mu_\theta = 3 - \omega_p^2/\omega^2$, and $\epsilon = 1$, in a free space background. The cylinder has a radius of $16\lambda_p$, where $\lambda_p = 2\pi c/\omega_p$. A current sheet, $\mathbf{J} = \exp(-(y - 6\lambda_p)^2/(3\lambda_p)^2)\delta(x - 20\lambda_p)\hat{z}$, carrying two frequencies, $\omega_1 = 0.6\omega_p$ and $\omega_2 = 0.65\omega_p$, is put in a free space background. At ω_1, $\mu_\theta = 0.2222$, resulting in $\alpha = 0.4715$; at ω_2, $\mu_\theta = 0.6331$, resulting in $\alpha = 0.7957$. Thus, $\Delta\theta^\alpha(\omega_1) = 0.4715\Delta\theta^s$ and $\Delta\theta^\alpha(\omega_2) = 0.7957\Delta\theta^s$. The simulated power flow is plotted in Fig. 2. It is seen that EM waves at different

Table 1. α-Relation between a Diagonal Anisotropic Medium and an Isotropic Medium[a]

Propagation Plane	Polarization	Anisotropic Media	α-relation	Isotropic Media
$x^1 - x^2$	TE	μ_{x^1} μ_{x^2} ϵ_{x^3}	$\alpha = \mathrm{sgn}\sqrt{\mu_{x^2}/\mu_{x^1}}$	$n = \sqrt{\epsilon_{x^3}\mu_{x^1}}$
	TM	ϵ_{x^1} ϵ_{x^2} μ_{x^3}	$\alpha = \mathrm{sgn}\sqrt{\epsilon_{x^2}/\epsilon_{x^1}}$	$n = \sqrt{\mu_{x^3}\epsilon_{x^1}}$
$x^1 - x^3$	TE	μ_{x^1} μ_{x^3} ϵ_{x^2}	$\alpha = \mathrm{sgn}\sqrt{\mu_{x^3}/\mu_{x^1}}$	$n = \sqrt{\epsilon_{x^2}\mu_{x^1}}$
	TM	ϵ_{x^1} ϵ_{x^3} μ_{x^2}	$\alpha = \mathrm{sgn}\sqrt{\epsilon_{x^3}/\epsilon_{x^1}}$	$n = \sqrt{\mu_{x^2}\epsilon_{x^1}}$

[a]All material components of the anisotropic medium have the same sign. sgn $= 1$ when the material parameters are positive, and sgn $= -1$ when they are negative. *The validity of this table requires that α and $n^2 g^c$ be independent of x^2 and x^3, where g^c is the metric tensor of the coordinates (x^1, x^2, x^3) in the laboratory space.*

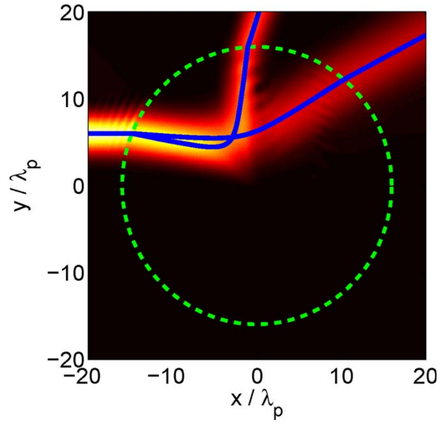

Fig. 2. (Color online) Simulated power flow for a current sheet, $\mathbf{J} = \exp(-(y - 6\lambda_p)^2/(3\lambda_p)^2)\delta(x - 20\lambda_p)\hat{z}$, with two frequencies, $\omega_1 = 0.6\omega_p$ and $\omega_2 = 0.65\omega_p$, interacting with a cylinder in free space. The cylinder has material parameters $\mu_r = 1$, $\mu_\theta = 3 - \omega_p^2/\omega^2$, and $\epsilon = 1$, and has a radius of $16\lambda_p$, where $\lambda_p = 2\pi c/\omega_p$. The dashed circle represents the boundary of the cylinder. The solid curves represent the calculated light ray from Eq. (6) based on the light ray in the corresponding isotropic seed medium.

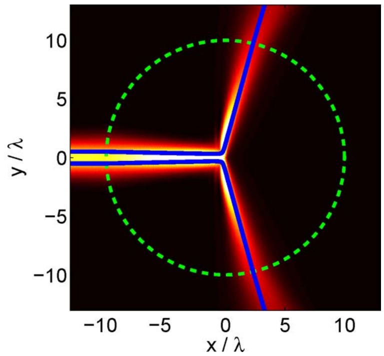

Fig. 3. (Color online) Simulated power flow for a current sheet, $\mathbf{J} = \exp(-y^2/(2\lambda)^2)\delta(x - 11\lambda_p)\hat{z}$, at wavelength λ, interacting with a cylinder in free space. The cylinder has material parameters $\mu_r = 3$, $\mu_\theta = 1$ and $\epsilon = 1$, with a radius of 10λ. The dashed circle represents the boundary of the cylinder. The solid curves represent the calculated light ray from Eq. (6) based on the light ray in the corresponding isotropic seed medium.

frequencies are rotated by different angles. In other words, the cylinder operates as a frequency demultiplexer. Here it should be noticed that the dispersive μ_θ is always associated with a material loss, which can degrade the performance of such a frequency demultiplexer. Thus, in practice, it is always desirable to design μ_θ with a small loss.

B. Beam Splitter

A beam splitter is an optical device that splits one beam into two or more. Here it is shown that the α media can be used as a beam splitter over a broadband frequency range. One can first consider that a beam normally incidents on a cylinder from free space. The angular coordinate, where the beam enters the cylinder, is assumed to be around $\theta_0 = \pi$. The propagation direction of the incident beam is parallel with the x axis. If the cylinder is composed of only an isotropic medium, the beam leaves the cylinder around $\theta_1 = 0$ or $\theta_1 = 2\pi$. Thus, $\Delta\theta^s = \theta_1 - \theta_0 = \pm\pi$, where $\Delta\theta^s = \pi$ applies to the light ray just below $y = 0$, and $\Delta\theta^s = -\pi$ applies to the light ray just above $y = 0$. If the isotropic medium in the cylinder is replaced by the α medium, the angular change $\Delta\theta^\alpha$ is equal to $\pm\alpha\pi$ according to the α-relation. This indicates that the beam is split into two, provided that α is not an integer. As a result, the cylinder composed of the α medium can operate as a beam splitter. As an example, one chooses a cylinder composed of a medium with $\mu_r = 3$, $\mu_\theta = 1$, and $\epsilon = 1$. Obviously, such a medium is an α medium with $\alpha = 1/\sqrt{3}$, as seen in Table 1. For a beam normally entering the cylinder around $\theta_0 = \pi$, one knows that $\Delta\theta^\alpha = \pm\pi/\sqrt{3}$. Thus, the beam is split equally into $\theta_1 = \pi + \pi/\sqrt{3}$ and $\theta_1 = \pi - \pi/\sqrt{3}$. The simulated power flow distribution for a current sheet, $\mathbf{J} = \exp(-y^2/(2\lambda)^2)\delta(x - 11\lambda)\hat{z}$, at the wavelength λ, interacting with this cylinder of a radius of 10λ, is plotted in Fig. 3. Clearly, the beam is split in two by the cylinder, in agreement with the theory.

C. Focusing Lens

Consider a cylinder composed of free space put in a free space background. A plane wave from the left infinity incidents on such a cylinder. The light rays are plotted in Fig. 4(a). It is seen that the angular coordinates for each light ray entering and leaving the cylinder, denoted as θ_0 and θ_1, are symmetric with respect to the dashed line, i.e., the y axis. Then, consider that free space inside the cylinder is replaced by an α medium, which has the α-relation with free space, and $\alpha = 1/2$. The corresponding light rays can be calculated from Eq. (6) based on the light rays in Fig. 4(a), and are plotted in Fig. 4(b). It is seen that, after passing through the cylinder, all light rays are focused on two points denoted as A_1 and A_2. To explain this focusing phenomenon, one notices that $\Delta\theta^\alpha = 1/2\Delta\theta^s = 1/2(\theta_1 - \theta_0)$, according to the α-relation. Then the light ray leaving the cylinder is at $\theta_1^\alpha = \theta_0 + \Delta\theta^\alpha = \theta_0/2 + \theta_1/2$, which corresponds to the angular coordinate of A_1 or A_2. Thus, the light rays are focused on A_1 and A_2. Considering the phase changes for the light rays crossing the cylinders in Figs. 4(a) and 4(b), one has $\Delta\phi^\alpha = 1/2\Delta\phi^s$. This implies that all light rays at the focusing points in Fig. 4(b) have the same phase, just like the light rays arriving the dashed line in Fig. 4(a). Thus, the cylinder in Fig. 4(b) really operates as a focusing lens. Since only one-half of the cylinder interacts with the light rays as seen in Fig. 4(b), the same lensing effect can be realized with a half structure.

To demonstrate this application, we consider a cylinder composed of a medium with $\mu_r = 2$, $\mu_\theta = 1/2$, and $\epsilon = 1/2$, which is just an ideal α medium with $\alpha = 1/2$ and $n = 1$ for TE polarization, as seen in Eq. (10). Of course, there are other options to choose for simplified α media, such as $\mu_r = 1$, $\mu_\theta = 1/4$, and $\epsilon = 1$. The reason why we choose the ideal α medium is that this medium has a better impedance matching

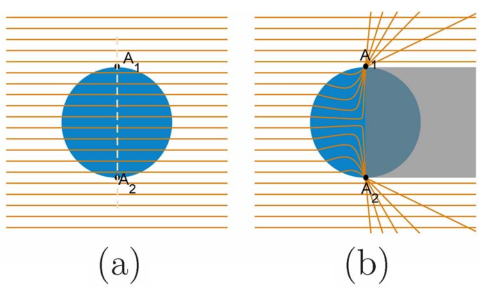

Fig. 4. (Color online) Illustration of light rays for a plane wave from the free space background interacting with a cylinder composed of (a) free space, (b) an α medium, which has the α-relation with free space, and $\alpha = 1/2$. In (b), the reflected rays are not plotted.

with the free space background. In the simulation, the cylinder is chosen to have the same radius as that in Fig. 3. The simulated electric field intensity distribution for a TE plane wave interacting with the cylinder is plotted in Fig. 5(a). It is clearly seen that the plane wave is focused on two points. Also, the field intensity at the focusing point is enhanced nearly 20 times compared with the incident field intensity. In Fig. 5(b), the simulated electric field intensity distribution for a TE plane wave interacting with the half-cylinder is plotted. The same focusing phenomenon is observed.

D. Radiation Controller

Consider that a line current source is put inside a cylinder and is located at (r_c, θ_c) with $r_c \neq 0$. The background is free space. If the cylinder is composed of free space, EM waves emit from the cylinder isotropically. This means that the angular coordinate denoted as θ_1 for the light ray leaving the cylinder has a range of $[0, 2\pi]$. Here the angular difference $\Delta\theta^s$ is defined as $\Delta\theta^s = \theta_1 - \theta_c$, which has a range of $[-\pi, \pi]$. Consider that the cylinder is composed of an α medium, which has the α-relation with free space. The angular coordinate for the light ray leaving the cylinder is denoted as θ_1^α. Then, the angular difference $\Delta\theta^\alpha$ is defined as $\Delta\theta^\alpha = \theta_1^\alpha - \theta_s$. It can be proved that $\Delta\theta^\alpha = \alpha\Delta\theta^s$, just as in the refraction case. Thus, $\Delta\theta^\alpha$ has a range of $[-\alpha\pi, \alpha\pi]$. Here it is noticed that, when $\alpha > 1$, the difference between the maximum and minimum values of $\Delta\theta^\alpha$ is larger than 2π. This indicates that the light rays emit from the cylinder in all directions and there are multiple rays leaving the cylinder at the certain angular location. When $\alpha < 1$, the difference between the maximum value and the minimum value of $\Delta\theta^\alpha$ is smaller than 2π. The light rays emit from the cylinder in a limited angular range. θ_1^α is equal to $\theta_c + \alpha\Delta\theta^s$. Thus, the angular range of the radiation can be controlled by tuning the parameters α and θ_c.

We numerically demonstrate this application by considering an example where a cylinder is composed of an α medium with the same material parameters as those in Fig. 5. The radius of the cylinder is 8λ. A line current source is put at $r_c = 4\lambda$, and $\theta_c = 0$. The simulated electric field distribution is plotted in Fig. 6(a1). It is seen that most radiated waves are limited in a range of $[-\pi/2, \pi/2]$, which agrees with our theory. The α medium in Fig. 6(a1) can be simplified to $\mu_r = 1$, $\mu_\theta = 1/4$, and $\epsilon = 1$. The simplified medium has only one material component smaller than 1 and is therefore much easier to fabricate. The simulated electric field distribution for the same source as in Fig. 6(a1) interacting with such a simplified α medium is plotted in Fig. 6(a2). It is seen that most radiated waves are still limited in the angular range of $[-\pi/2, \pi/2]$. However, compared with Fig. 6(a1), noticeable radiated waves are observed in the angular range of $[\pi/2, 3\pi/2]$, due to the reflections induced at the cylinder boundary. In Fig. 6(a3), the radiation power, normalized by the power from the same source put in free space for Figs. 6(a1) and 6(a2), is plotted. Clearly, most power is limited in the angular range of $[-\pi/2, \pi/2]$. Next, we consider that the α medium has material parameters $\mu_r = 4/3$, $\mu_\theta = 3/4$, and $\epsilon = 3/4$. Obviously, in this case, the parameter α is equal to $3/4$. The same line current source as in Figs. 6(a1) and 6(a2) is put inside the cylinder. According to the theory, the radiated waves are limited in an angular range of $[-3\pi/4, 3\pi/4]$. The simulated electrical field distribution is plotted in Fig. 6(b1), which agrees with the theory. Then, we simplify the α medium to $\mu_r = 1$, $\mu_\theta = 9/16$, and $\epsilon = 1$. The corresponding electric field distribution is plotted in Fig. 6(b2). The same phenomenon is also observed. In Fig. 6(b3), the normalized radiation power is plotted for Figs. 6(b1) and 6(b2).

6. REVISITING INVISIBILITY CLOAKS

In this section, we will revisit invisibility cloaks [1], derived traditionally from the coordinate transformation . The working mechanism of such cloaks will be interpreted qualitatively from the perspective of α transformation media. Let us first consider a linearly transformed cylindrical cloak with material parameters

$$\epsilon_r = \mu_r = \frac{r-a}{r}, \qquad \epsilon_\theta = \mu_\theta = \frac{r}{r-a},$$
$$\epsilon_z = \mu_z = \left(\frac{b}{b-a}\right)^2 \frac{r-a}{r}, \tag{12}$$

where b and a represent the outer and inner radii of the cloak, respectively. We are interested in light propagating in the $r-\theta$ plane. According to Table 1, the invisibility cloak can be considered an α medium, which has the α relationship with an isotropic seed medium. The refractive index n of such an isotropic medium and the parameter α are expressed as

$$n = \frac{b}{b-a}\frac{r-a}{r}, \qquad \alpha = \frac{r}{r-a}. \tag{13}$$

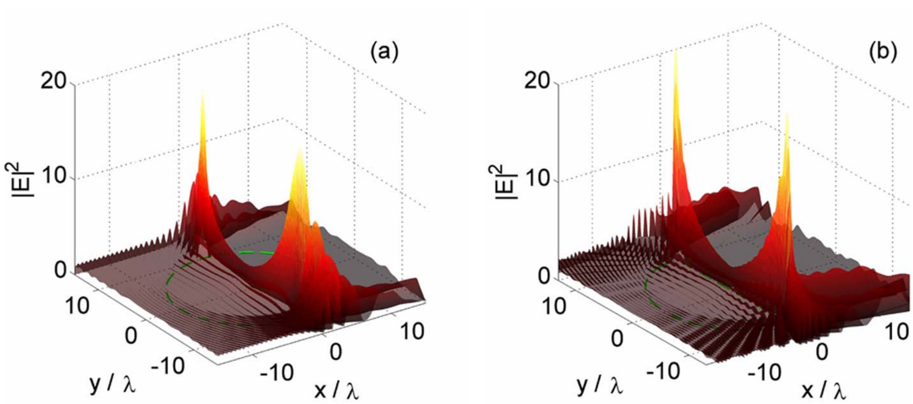

Fig. 5. (Color online) Simulated electric field intensity for a TE plane wave interacting with (a) a cylinder; (b) the half-cylinder. The cylinder has material parameters $\mu_r = 2$, $\mu_\theta = 1/2$ and $\epsilon = 1/2$, and has a radius of 10λ. The background is free space. The dashed circle represents the boundary of the cylinder or the half-cylinder.

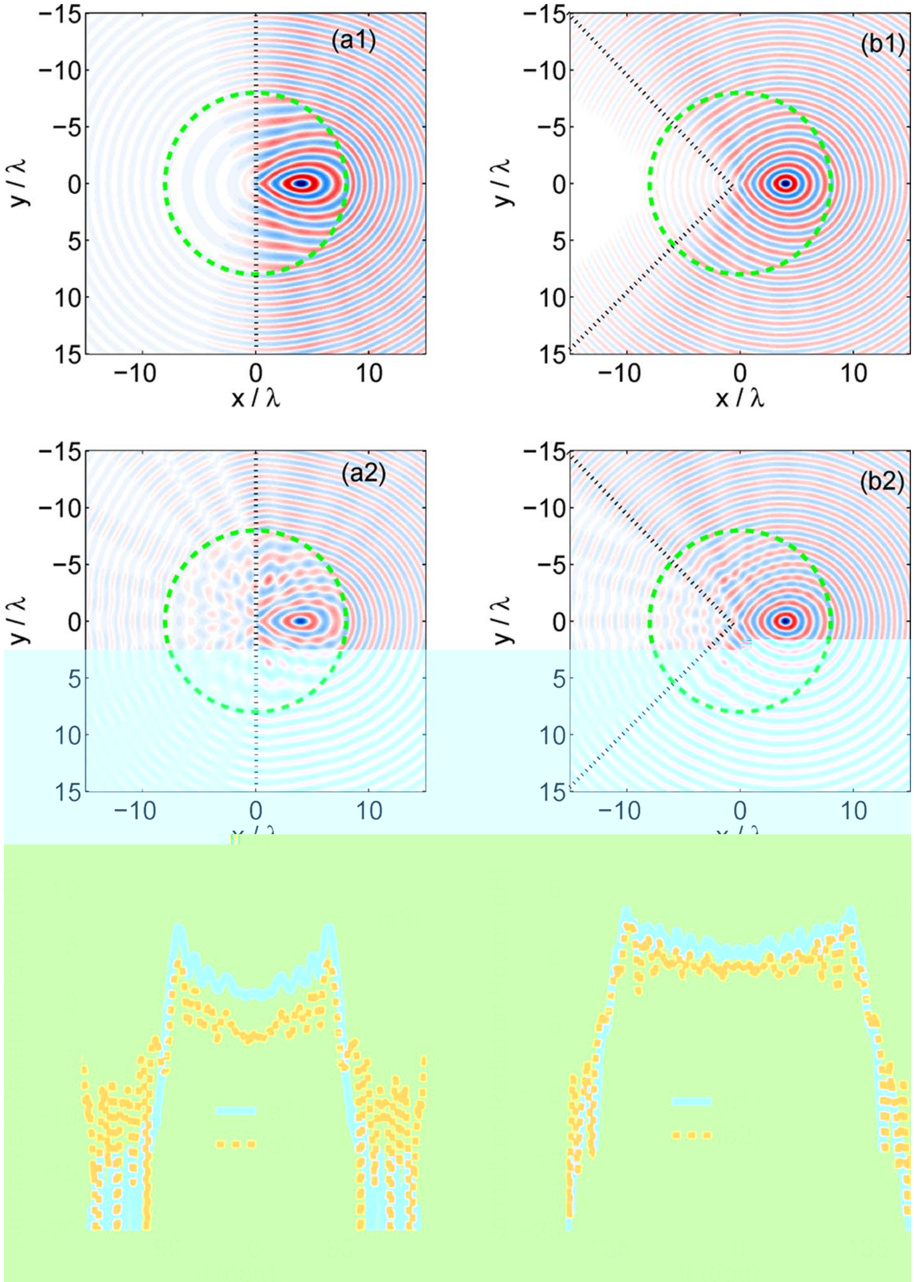

Fig. 6. (Color online) Simulated electric field distribution for a line current at $r_c = 4\lambda$ and $\theta_c = 0$ interacting with a cylinder composed of a medium with (a1) $\mu_r = 2$, $\mu_\theta = 1/2$, and $\epsilon = 1/2$; (a2) $\mu_r = 1$, $\mu_\theta = 1/4$, and $\epsilon = 1$; (b1) $\mu_r = 4/3$, $\mu_\theta = 3/4$, and $\epsilon = 3/4$; (b2) $\mu_r = 1$, $\mu_\theta = 9/16$, and $\epsilon = 1$. The normalized radiation power for (a1) and (a2) is plotted in (a3). The normalized radiation power for (b1) and (b2) is plotted in (b3). The cylinder has a radius of 8λ. The dashed line in (a1), (a2), b(1) and (b2), represents the boundary of the cylinder. The dotted line in all figures represents the boundary of the radiation range from our theory.

Consider the light ray in an isotropic shell $a \le r \le b$, with a refractive index of n in Eq. (13). As seen from Eq. (13), n decreases gradually from 1 to 0 as r varies from $r = b$ to $r = a$. When $n = 0$, the medium has a zero optical volume. This indicates that the light ray feels the boundary $r = a$ as an optical point. Thus, the light ray cannot enter the region inside the boundary $r = a$, as seen in Fig. 7(a). The light rays in Fig. 7(a) are obtained by a numerical ray-tracing. According to the α-relation between the cloak and such an isotropic shell, it can be deduced that the light ray also cannot enter the region enclosed by the cloak. Observing the rotation

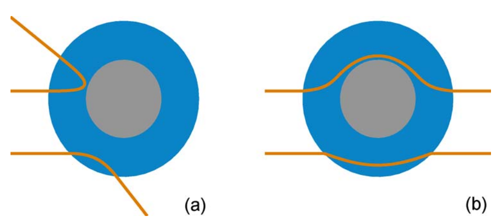

Fig. 7. (Color online) Illustration of light rays passing through (a) an isotropic shell with a refractive index of $\frac{b}{b-a}\frac{r-a}{r}$; (b) a cylindrical invisibility cloak with material parameters from Eq. (12). The invisibility cloak in (b) has the α-relation with the isotropic shell in (a). The background is free space.

parameter α, it is seen that α increases from $b/(b-a)$ to $+\infty$ as r varies from $r=b$ to $r=a$. This indicates that the light rays experience a sharp rotation near the inner boundary of the cloak. This also qualitatively explains why the light ray can bypass the cloaked region enclosed by $r=a$ and rotate back to its original direction, even in the case in which the light ray is incident on the cloak near normally. By using Eq. (5), the light rays in the invisibility cloak are plotted in Fig. 7(b) based on those in Fig. 7(a).

Consider a linearly transformed spherical cloak, which has material parameters $\epsilon_r=\mu_r=\left(\frac{r}{r-a}\right)^2\frac{b}{b-a}$, $\epsilon_\theta=\epsilon_\varphi=\mu_\theta=\mu_\varphi=\frac{b}{b-a}$. Obviously, the spherical cloak is an α medium, which has the same n and α as the cylindrical case in Eq. (13). Thus, the above qualitative understanding for the cylindrical cloak can similarly be applied here.

7. CONCLUSION

In the present paper, we construct a type of transformation medium for manipulating light by an approach different from the coordinate transformation. The construction process starts from a space called seed space with the corresponding transformation media called seed media. Applying a direct transformation to the metric tensor of the seed space, another space, called α space, is obtained, with the corresponding transformation media called α media. The transformation relation correlates the metric tensors of two spaces by either a constant or a function denoted as α. Unlike the coordinate transformation approach, two transformation media or spaces can have different curvature properties. Light trajectories in the seed and α media have a simple displacement or rotation relationship called the α-relation, determined by the parameter α. The phase changes of the light ray passing through the two media are different, which connect to each other through the parameter α. This property also characterizes the difference between our approach and the coordinate transformation approach. The concept of α media covers three types of commonly experienced anisotropic media: (1) respecting continuous translational symmetry concerning two Cartesian coordinate components and having a slab shape; (2) respecting cylindrical rotational and continuous longitudinal translational symmetry and having a cylindrical shape; (3) respecting spherical rotational symmetry and having a spherical shape, with two principal axes along the symmetry directions and material parameters having the same sign. Such anisotropic media relate to certain isotropic media as their seed media. To illustrate the applications of the α media, several optical devices, such as a frequency demultiplexer, beam splitter, focusing lens, and radiation controller, are proposed. The mechanism of invisibility cloaks traditionally derived from the coordinate transformation are revisited by treating them as α media.

APPENDIX A: PROOF OF EQ. (5)

To prove that Eq. (5) is the refracted light ray equation when the seed medium is replaced by the α medium, we take two steps. In the first step, we prove that Eq. (5) describes a geodesic (line with extremum length). The light ray should follow the geodesic. In the second step, we prove that Eq. (5) also satisfies the corresponding boundary conditions.

First step: The geodesic is the curve with the extremum length between two points. The length of a line in a space is defined as

$$s=\int \mathrm{d}s=\int L\mathrm{d}\sigma, \tag{A1}$$

where σ is an arbitrary parameter, and L is the "Lagrangian" expressed as

$$L=\sqrt{g_{ij}\frac{dx^i}{d\sigma}\frac{dx^j}{d\sigma}}. \tag{A2}$$

The geodesic requires that the first-order variation to the length be zero, which is equivalent to the Euler–Lagrange equation

$$\frac{d}{d\sigma}\frac{\partial L}{\partial(dx^i/d\sigma)}=\frac{\partial L}{\partial x^i}=0. \tag{A3}$$

The Lagrangians of the seed medium and the α medium are denoted as L^s and L^α, respectively. Because Eq. (4) is the equation of the refracted light ray in the seed medium, we can set Eq. (4) to be a solution to Eq. (A3). Substituting the right side of Eq. (4) into Eq. (A3), three equations can be obtained. As an example, one equation concerning $x^i=x^1$ is expressed as

$$\frac{d}{d\sigma}\frac{g^s_{1i}\frac{df_i(\sigma)}{d\sigma}}{L^s}-\frac{1}{2L^s}\frac{\partial g^s_{ij}}{\partial x^1}\frac{df_i(\sigma)}{d\sigma}\frac{df_j(\sigma)}{d\sigma}=0. \tag{A4}$$

Substituting the right side of Eq. (5) into the left side of the Euler–Lagrange
equation, three expressions denoted as A_i $(i=1,2,3)$ are obtained. The expression A_1 concerning $x^i=x^1$ is found to be

$$A_1=\alpha(x_1)\left(\frac{d}{d\sigma}\frac{g^s_{1i}\frac{df_i(\sigma)}{d\sigma}}{L^s}-\frac{1}{2L^s}\frac{\partial g^s_{ij}}{\partial x^1}\frac{df_i(\sigma)}{d\sigma}\frac{df_j(\sigma)}{d\sigma}\right). \tag{A5}$$

From Eq. (A4), we derive that $A_1=0$. Similarly, we derive that $A_2=A_3=0$. Thus, it has been proved that Eq. (5) describes a geodesic equation in the α medium.

Second step: The point where the light ray enters the seed medium is at $(f_1(\sigma_1),f_2(\sigma_1),f_3(\sigma_1))$. When the seed medium is replaced by the α medium, it is required the refracted light ray also pass the point $(f_1(\sigma_1),f_2(\sigma_1),f_3(\sigma_1))$, because the incident ray is not changed. Observing Eq. (5), this boundary condition is automatically satisfied.

The other boundary condition concerns the conservation of momentum. To demonstrate this boundary condition, the Hamiltonian of the light ray in the seed medium is introduced:

$$H=g^{sij}k^s_ik^s_j=\frac{\omega^2}{c^2}, \tag{A6}$$

where $k^s_i=d\phi^s/dx^i$, ϕ^s is the phase of the light, and $g^{sij}=(g^s_{ij})^{-1}$. At $(f_1(\sigma_1),f_2(\sigma_1),f_3(\sigma_1))$, the wave vector is denoted as k^{sc}_i. When the seed medium is replaced by the α medium, the new Hamiltonian is obtained by replacing g^{sij} with $g^{\alpha ij}$ in Eq. (A6), where $g^{\alpha ij}=(g^\alpha_{ij})^{-1}$. Similarly, the wave vectors k^α_i in the α transformation medium can be defined. At

$(f_1(\sigma_1), f_2(\sigma_1), f_3(\sigma_1))$, the wave vector is denoted as $k_i^{\alpha c}$. Because the same light ray incidents on the seed medium and the α medium from the same background, it is required that $k_2^{sc} = k_2^{\alpha c}$ and $k_3^{sc} = k_3^{\alpha c}$. This boundary condition is proved to be satisfied in the following discussion.

Equation (A6) can be reduced to a set of ordinary differential equations:

$$\frac{dx^i}{d\tau} = 2g^{sij}k_j^s, \tag{A7}$$

$$\frac{dk_i}{d\tau} = -\frac{dg^{sjl}}{dx^i}k_j^s k_l^s. \tag{A8}$$

From Eqs. (A7) and (A8), the light ray equation can also be derived. Thus, the Hamiltonian approach is equivalent to the previous Lagrangian approach. Connecting two approaches by the Legendre transformation, it is derived that

$$\frac{k_i^s}{k_j^s} = \frac{g_{il}^s \frac{dx^l}{d\sigma}}{g_{jl}^s \frac{dx^l}{d\sigma}}. \tag{A9}$$

Similarly, for the α medium, we have

$$\frac{k_i^\alpha}{k_j^\alpha} = \frac{g_{il}^\alpha \frac{dx^l}{d\sigma}}{g_{jl}^\alpha \frac{dx^l}{d\sigma}}. \tag{A10}$$

From Eqs. (A9) and (A10), it is derived that

$$\frac{k_1^\alpha}{k_3^\alpha} = \alpha\frac{k_1^s}{k_3^s}, \qquad \frac{k_2^\alpha}{k_3^\alpha} = \frac{k_2^s}{k_3^s}. \tag{A11}$$

With Eq. (A11) and the Hamiltonians for the seed medium and the α medium, we derive that

$$k_1^\alpha = \alpha k_1^s, \qquad k_2^\alpha = k_2^s, \qquad k_3^\alpha = k_3^s. \tag{A12}$$

Equation (A12) naturally implies that the boundary condition of $k_2^{sc} = k_2^{\alpha c}$ and $k_3^{sc} = k_3^{\alpha c}$ is satisfied. Thus, Eq. (5) is proved to be the correct light ray when the seed medium is replaced by the α transformation medium.

APPENDIX B: DERIVATIONS TO EQ. (8)

It is known that the phase change in the medium is proportional to the geodesic length defined in Eq. (A1). In particular, one has

$$\Delta\phi = \frac{\omega}{c}\int_{\sigma_1}^{\sigma_2} L\mathrm{d}\sigma. \tag{B1}$$

For the seed medium and the α medium, the phase changes are denoted as $\Delta\phi^s$ and $\Delta\phi^\alpha$, respectively. Writing the Lagrangians down and taking the expressions into Eq. (B1), it is found that

$$\Delta\phi^s = \frac{\omega}{c}\int_{\sigma_1}^{\sigma_2} L^s\mathrm{d}\sigma, \qquad \Delta\phi^\alpha = \frac{\omega}{c}\int_{\sigma_1}^{\sigma_2} \alpha(x^1)L^s\mathrm{d}\sigma. \tag{B2}$$

When α is a constant, it is derived that

$$\Delta\phi^\alpha = \alpha\Delta\phi^s, \tag{B3}$$

i.e., Eq. (8).

ACKNOWLEDGMENTS

This work is supported by the Swedish Foundation for Strategic Research (SSF) through the INGVAR program and the Swedish Research Council (VR).

REFERENCES

1. J. B. Pendry, D. Schurig, and D. R. Smith, “Controlling electromagnetic fields,” Science **312**, 1780–1782 (2006).
2. U. Leonhardt, “Optical conformal mapping,” Science **312**, 1777–1780 (2006).
3. U. Leonhardt and T. G. Philbin, “General relativity in electrical engineering,” New J. Phys. **8**, 247 (2006).
4. U. Leonhardt and T. G. Philbin, “Transformation optics and the geometry of light,” Prog. Opt. **53**, 69–152 (2009).
5. M. Yan, W. Yan, and M. Qiu, “Invisibility cloaking by coordinate transformation,” Prog. Opt. **52**, 261–301 (2009).
6. Z. C. Ruan, M. Yan, C. W. Neff, and M. Qiu, “Ideal cylindrical cloak: perfect but sensitive to tiny perturbations,” Phys. Rev. Lett. **99**, 113903 (2007).
7. H. S. Chen, B. I. Wu, B. L. Zhang, and J. A. Kong, “Electromagnetic wave interactions with a metamaterial cloak,” Phys. Rev. Lett. **99**, 063903 (2007).
8. D. Schurig, J. J. Mock, B. J. Justice, S. A. Cummer, J. B. Pendry, A. F. Starr, and D. R. Smith, “Metamaterial electromagnetic cloak at microwave frequencies,” Science **314**, 977–980 (2006).
9. J. Valentine, J. Li, T. Zentgraf, G. Bartal, and X. Zhang, “An optical cloak made of dielectrics,” Nat. Mater. **8**, 568–571 (2009).
10. L. H. Gabrielli, J. Cardenas, C. B. Poitras, and M. Lipson, “Silicon nanostructure cloak operating at optical frequencies,” Nat. Photon. **3**, 461–463 (2009).
11. Y. Lai, H. Y. Chen, Z. Q. Wang, and C. T. Chan, “Complementary media invisibility cloak that cloaks objects at a distance outside the cloaking shell,” Phys. Rev. Lett. **102**, 093901 (2009).
12. A. Greenleaf, Y. Kurylev, M. Lassas, and G. Uhlmann, “Electromagnetic wormholes and virtual magnetic monopoles from metamaterials,” Phys. Rev. Lett. **99**, 183901 (2007).
13. W. Yan, M. Yan, and M. Qiu, “Achieving perfect imaging beyond passive and active obstacles by a transformed bilayer lens,” Phys. Rev. B **79**, 161101 (2009).
14. M. Yan, W. Yan, and M. Qiu, “Cylindrical superlens by a coordinate transformation,” Phys. Rev. B **78**, 125113 (2008).
15. M. Tsang and D. Psaltis, “Magnifying perfect lens and superlens design by coordinate transformation,” Phys. Rev. B **77**, 035122 (2008).
16. Y. Lai, J. Ng, H. Y. Chen, D. Z. Han, J. J. Xiao, Z. Q. Wang, and C. T. Chan, “Illusion optics: The optical transformation of an object into another object,” Phys. Rev. Lett. **102**, 253902 (2009).
17. Y. G. Ma, C. K. Ong, T. Tyc, and U. Leonhardt, “An omnidirectional retroreflector based on the transmutation of dielectric singularities,” Nat. Mater. **8**, 639–642 (2009).
18. L. Bergamin, “Generalized transformation optics from triple spacetime metamaterials,” Phys. Rev. A **78**, 043825 (2008).